Achieving Axial Balance of a Microturbine Rotor with Low Bearing Pressures for Start-up and High Speed Operation

Félix Gauthier[1], Changgu Lee[2], Luc Fréchette[1]

[1] Université de Sherbrooke, Department of Mechanical Engineering
2500 boul. Universite, Sherbrooke, QC, J1K 2R1, Canada
[2] Columbia University, Department of Mechanical Engineering
220 Mudd bldg, MC 4703, New York, NY 10027, USA

Abstract

Modelization of the pressure field around a 4mm diameter rotor of a microturbine was done to see the interaction between the components (multistage microturbine, spiral groove viscous seals and pump, hydrostatic bearings) and there impact on axial force and stiffness to achieve low thrust bearing axial balance. A new operating configuration was explored experimentally to balance axial force on the rotor while reducing the pressure of the thrust bearing to only few psig. Investigation on a possible way of feeding the thrust bearing from the turbine inlet flow suggests that a microturbine Rankine device with hydrostatic bearings could be operated in a self-sustained manner, without the need for externally pressurized gases.

Keyword : Microturbine, Microrotor, Gas bearings, Thrust bearings, Axial stiffness

1 – INTRODUCTION

Since nearly a decade, silicon microturbines have been under development as a promising approach for portable power generation [1, 2]. A key challenge consists of operating the millimeter scale rotors at very high rotational speeds (> $1x10^6$ RPM). Proper operation requires that the forces and moments on the rotor, applied by the supporting air bearings, be well balanced to prevent physical contact of the silicon rotor with the surrounding structure. Although recent work on microturbine components significantly improves our understanding of the rotor dynamics and principles of operation [3, 4], every new configuration requires a detailed study. Of interest here is the micro turbopump device with a multi-stage turbine and viscous pump supported on gas-lubricated bearings that was fabricated and demonstrated by Lee as the rotating subsystem for a micro Rankine power system [2, 5]. The device consists of a 4mm diameter turbine disk enclosed in a stack of five micromachined wafers created by deep reactive ion etching and wafer bonding. The goal of the present study is to define the forces on the rotor to operate the actual device, and future generation of it, in a proper manner from start-up to high speed operation, accounting for fabrication issues and constraints.

2 - DEVICE DESCRIPTION

This section introduces the microturbine device and describes the components that influence the pressure field around the rotor following the illustration of Fig. 1. To have precise detail on geometric features, refer to Lee [6]. The turbine, seals and bearings are designed to work with gas (air or steam) and the pump with liquid (water). The turbine (*a*) is composed of 4 interlaced rows of stator and rotor blades that induce a rotation of the rotor as a pressurized gas flows through (from port 1 to port 2). This motion creates a liquid flow through the spiral groove viscous pump (*d*) on the back side or the rotor (between ports 4 and 5, depending on the orientation of the spiral grooves). A pair of hydrodynamic spiral groove seals (*b, e*) keeps the liquid in the center of the device. In the center of the rotor, geometric features permit measurement of the rotor speed with an optical probe.

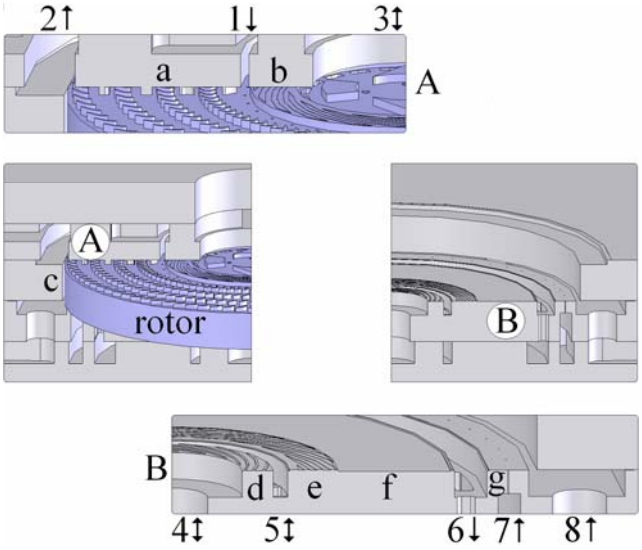

Figure 1 - Components around the rotor ; turbine (*a*), top seal (*b*), journal bearing (*c*), pump (*d*), bottom seal (*e*), axial balance plenum (*f*) and peripheral thrust bearing (*g*). Numbers are referring to different ports where flows can come in or out. On B view, the rotor and the two top layers are removed.

The axial balance plenum (*f*) is composed of a large flat area over which the pressure can be varied to balance the axial forces on the rotor. A peripheral hydrostatic thrust bearing (*g*) is also designed to produce a counteracting force and provide axial and tilt stiffness. Flow is supplied through port 7, goes through a circular array of small orifices, then exits by port 6 and through the journal bearing. Radial support of the rotor is provided by the hydrostatic journal bearing (*c*), which consists of a narrow gap surrounding the rotor, pressurized with flow from port 8 that then joins the turbine exit flow. As the supplied flow goes through the journal bearing, it encounters a pressure loss (entry and viscous) that depends on the local gap. The pressure profile induced along the journal bearing gap is such that a restoring force results from a radial movement of the rotor.

Problematic - During past experiments [6], the operating speed of the device was limited to 330,000 RPM due to insufficient bottom side pressure to balance the axial force on the turbine side. Also, the analytical force balance model was only valid for a limited number of port configurations. Since there are many ports on the device, a more complete model to simulate the impact of closing or opening of the different ports, including the interaction between components, was needed to evaluate alternate port configurations that would improve the axial balance since it was a probable cause of failure.

3- MODELING APPROACH

To achieve force and moment balance on the rotor, the pressure fields are iteratively calculated while changing the axial and tilt position of the rotor. Iteration on mass flows is done to match imposed port pressures and angular and radial discretization was done to take in account the geometry changes as the rotor move. The interaction between each component was simulated by imposing the same boundary conditions. This section briefly describes the component models and results of our analytical investigations.

3.1 - Components models

Turbine (*a* in Fig. 1) - For the pressure profile across the turbine, an empirical model was built from the experimental results of Lee [6]. It was found that the pressure profile scales up with the pressure differential across the turbine. Similarly for the rotational speed, a relation was established based on the pressure differential across the turbine and the experimental speed measurement.

Hydrodynamic spiral groove seal (*b* and *e* in Fig. 1) - The model for the top and bottom side seals is based on the work of Muijderman [7], referred to as a partially grooved flat thrust bearing. To take into account compressibility an iterative process was done to obtain mean properties. The model also includes a contraction and expansion lost at both end of the seals [6].

Hydrodynamic spiral groove viscous pump (*d* in Fig. 1) – Since Lee already demonstrated the pump [5], the experimental test of the present study does not involve water. The variation of the pressure field by the pump with air was found to be negligible upon investigation.

Axial balance plenum (*f* in Fig 1) - This component is modeled by a fully developed laminar compressible radial flow with contraction and expansion losses (based on CFD simulations [6]) for the annular restriction.

Peripheral hydrostatic thrust bearing (*g* in Fig 1) - For the thrust bearing, the model is based on the work of Deux [8] and Lee [6]. This is a series of orifice flow, fully developed laminar compressible radial flow, pressure lost (expansion and turning) and an adaptation factor to take the non uniformity of the pressure field into account as it reach both ends of the bearing [6]. In the event of chocked flow at the end of the orifices, a correction factor was introduced to match the outlets pressures.

3.2 - Configuration possibilities

Referring to Fig. 1, ports 3, 4 and 6 could be closed or opened during testing (since investigation of the pump flows shows no significant pressure variation while using gas, port 5 was not simulated). With the experimental apparatus, it is possible to impose a static pressure or a flow rate at any given port.

3.3 -Analytical investigation

The goal of this analysis is to present a new way of operating the device to solve the axial balance problem introduced at the end of section 2.

Resolving axial force balance problem - Even if the thrust bearing pressure was on the order of 100 psig [6], insufficient axial bottom force was encountered in pasts experiments and led to crashing problems at speed up to 330 000 RPM. Since central ports were open (4, 5 and 6 from Fig. 1) in these experiments, the upward force was only over the peripheral thrust bearing area. The solution proposed here is to use the entire area on the bottom side so the pressure can be reduced for the same total force. This is simply done by closing central ports 4, 5 and 6, which leads to a sufficient axial force while reducing the feed pressure of the auxiliary thrust bearing considerably. For example, these are the feeding thrust bearing pressures for an equivalent force of 0.15 N:

87 psig (past configuration) → 2 psig (new configuration)

Since, the model does not take into account all the 3D effects, we expect the pressure of the peripheral thrust bearing to be slightly higher but much lower than with the past configuration. The force from the bottom of the rotor could change form two principals parameters: the thrust bearing gap and feed pressure. Figures 2 and 3 show, respectively, axial force and axial stiffness produced by the thrust bearing for our new configuration. The axial stiffness was computed by the

ratio of the change of force for an imposed change of position and there seams to be an optimal thrust bearing gap as the inlet pressure rises. This behavior has also been noticed by Teo [3]. Compared with the previous configuration, we reduced considerably the thrust bearing inlet pressure while raising the force. The tilt stiffness was also calculated and shows similar behavior as the axial stiffness since it depends on local thrust bearing gap.

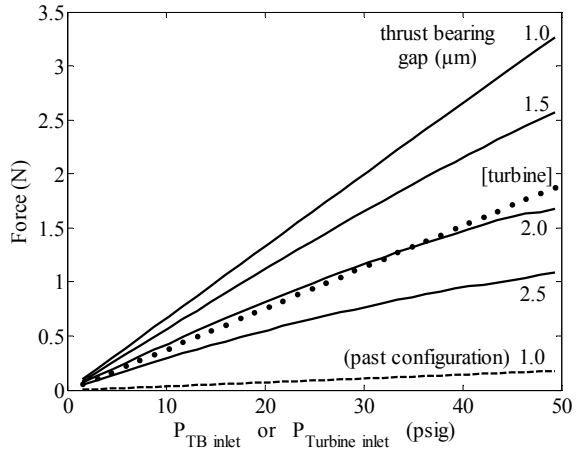

Figure 2 - Relative force produced on the bottom of the rotor for the new configuration (ports 4, 5 and 6 closed) compared to the past configuration (dashed lines, ports 4, 5 and 6 open). The dotted line is the downward turbine force as a function of its inlet pressure. Keeping the thrust bearing gap under 2μm leads to a lower inlet pressure for the thrust bearing compared to the turbine.

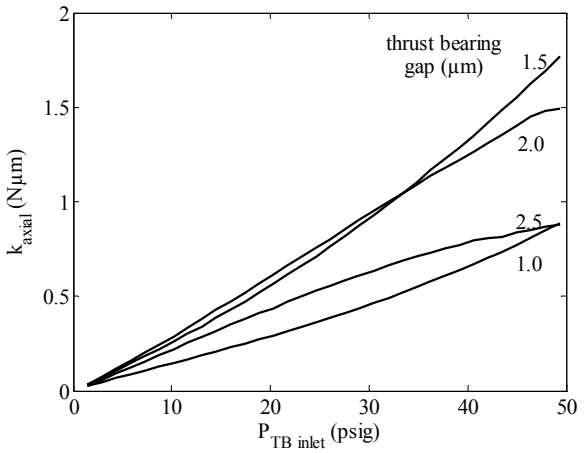

Figure 3 - Axial stiffness produced by the pressure field under the rotor for the new configuration proposed (ports 4, 5 and 6 closed).

Lowering thrust bearing pressure - Since the pressure profile on the top side of the rotor simply scales with the pressure differences across the turbine, it was found that the force could be evaluated by Eqn 1 where, for our geometry, $c = 5.53 \times 10^{-6}$ N/Pa, $d = 7.04 \times 10^{-6}$ N/Pa. Since practically all the bottom of the rotor is pressurised with the new port configuration, the force under the rotor could be evaluated simply by a uniform pressure. This way, only one pressure tap on the bottom could be used to control the bottom force by adjusting the feed pressure of the peripheral thrust bearing according to the turbine inlet and outlet pressures :

$$F_{top} = c \cdot P_{rel.\ in} + d \cdot P_{rel.\ out} \quad (1)$$

As shown in Fig. 2, the analysis suggests that the thrust bearing can be operated at pressures equal or lower than the turbine inlet pressure, for low turbine exit pressures (near ambient).

Tilt angle produced by misalignment of the bottom layer - During the fabrication, bottom layers were misaligned, resulting in a displacement of the pressure field on the bottom of the rotor that can produce tilting. A misalignment of few tens of microns would be sufficient to produce a non negligible tilt angle of the rotor. To reduce the tilt angle, especially at start-up, it is preferable to minimise misalignment, elevate the thrust bearing pressure, and maintain the rotor centered in the journal bearing. In a practical system however, the hydrostatic bearing flows are extracted from the turbine inlet flow, so the pressures are naturally limited.

4 – EXPERIMENTAL INVESTIGATION

The test apparatus used to operate the device (designed and fabricated by Lee [6]) is composed of a series of valves, mass flow controllers/meters, pressure sensors, piping and an optical sensor for speed measurement. The control and data acquisition was done using Labview.

4.1 – Validation of the new configuration at low speed

To validate the new port configuration for start-up, a simple starting test was done using low feed pressure in the thrust bearing. Figure 4 shows good agreement between test and model. The speed was lower then expected (24 kRPM vs 38 kRPM) and this is allowable to the fact that practically entire stator blades were missing (broken prior to this test) but even then, a rotor speed up to 200kRPM was achieved without problem. Starting up the rotation of the device found to be severely less complex with this new configuration. Since the thrust bearing exit flow end in the journal bearing entry, a starting procedure with no journal bearing flow was also proposed and experimentally validated.

4.2 – Self-sustained Hydrostatic Bearing Operation

For self-sustained operation of a practical microturbine device, the bearings should not require externally pressurized gas, but should instead bleed some gas from an internally pressurized source. For the proposed Rankine cycle, a small fraction of the turbine inlet flow (pressurized by the pump) would be used to support the rotor. The current investigation therefore aims at operating the hydrostatic thrust and journal bearings at pressures lower than the turbine inlet pressure. While journal bearing pressures have generally not exceeded 5 psig (turbine inlet pressures up to 30 psig), thrust bearings have required up to 100 psig.

This pressure can be significantly reduced by allowing the intermediate pressure in the thrust bearing (at the exit of the restrictors, before the radial gap) to act over the entire rotor surface; as with the new port configuration.

Further reduction can come by minimizing the pressure drop across the restrictors. For the current device, this was done by lowering the rotor to reduce the thrust bearing gap, which leads to a higher overall resistance and less bearing flow for fixed inlet and outlet thrust bearing pressures. Since the pressure under the rotor is closer to the TB feed pressure, a larger force is applied over the bottom of the rotor. This augmentation of the force allows a reduction of the thrust bearing inlet pressure. Figure 5 shows experimental and analytical results suggesting that it should be possible to operate hydrostatic bearings in a self-sustained manner for a micro Rankine device with the improved port configuration.

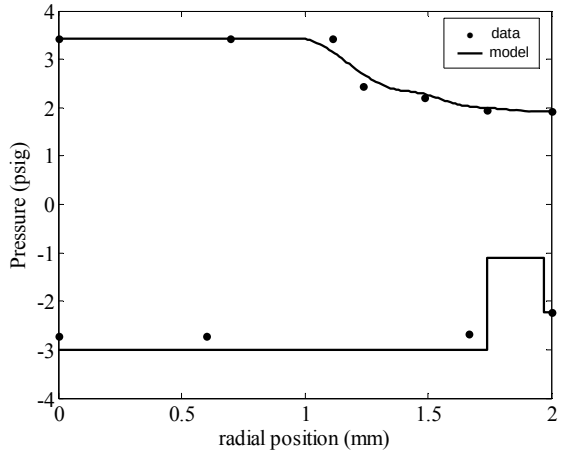

Figure 4 - Validation of the start-up procedure with low thrust bearing pressure (3.8psig). The rotor was stable and running at 24 500 RPM. The thrust gap for the analytical simulation was 2 μm.

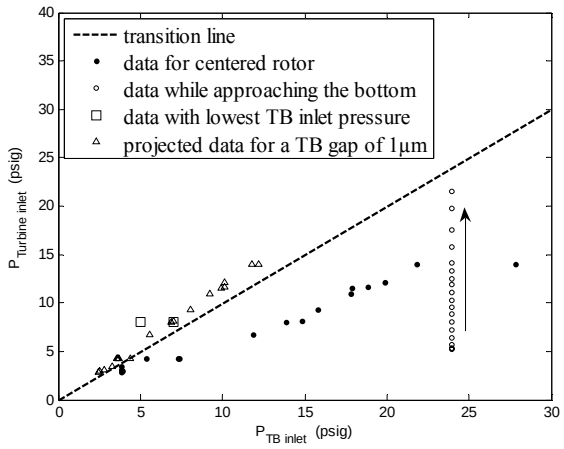

Figure 5 - Turbine versus thrust bearing inlet pressures. By reducing the thrust bearing gap, it is shown analytically and experimentally that the bearings can be operated with a single feed at the turbine inlet pressure.

5 - CONCLUSION

A new start-up procedure with low thrust bearing inlet pressure was established and experimental investigations have shown agreement with theory. With this configuration, it was possible to operate the device with minimal control (thrust bearing and turbine) to start the rotor spinning. Fabrication tolerance was estimated to avoid tilt unbalance due to misalignment of the bottom layer of the device. Investigation on the possibility of feeding the thrust bearing from the turbine inlet flow has been done and show promising result. With our new approach, it was possible to operate the device from few hundred of RPM to several thousand of RPM. High speed operation and journal bearing characterizations are underway.

ACKNOWLEDGMENTS

The work was supported by the Natural Sciences and Engineering Research Council of Canada (NSERC) and the Canada Research Chair programs. The device was developed with the support of NASA Glenn Res. Center (NAS3-03105, monitored by Dr. Glenn Beheim) and fabricated at the Cornell Nano. Sci. and Tech. facility (CNF), supported by NSF (ECS 03-35765). The authors acknowledge the support of Mokhtar Liamini for experimental procedures.

REFERENCES

[1] Fréchette, L.G. *et al.*, "High-Speed Microfabricated Silicon Turbomachinery and Fluid Film Bearings", J. of Microelectromech. Syst., Vol. 14, No. 1, pp141-152, 2005.

[2] Lee, C., Fréchette L.G., "Demonstration and Characterization of a Multi-stage Silicon Microturbine", Proc. ASME Int'l Mech. Eng. Congress & Expo., Orlando, Fl., Nov. 5-11, 2005, Paper IMECE2005-81435.

[3] Teo C.J., "MEMS Turbomachinery Rotordynamics: Modeling, Design and Testing", Ph.D thesis, M.I.T., June 2006.

[4] Liu L. X. "Theory for Hydrostatic Gas Journal Bearings for Micro-Electro-Mechanical Systems", Ph.D thesis, M.I.T., September 2005.

[5] Lee, C., Liamini M., Fréchette L.G., "Design, Fabrication, And Characterization of a Microturbopump for a Rankine Cycle Micro Power Generator", Solid State Sensors, Actuators and Microsystems Workshop, Hilton Head Island, SC., Jun. 4-8, 2006, p.276-279;

[6] Lee C., "Development of a Microfrabricated Turbopum for a Rankine Vapor Power Cycle", Ph.D thesis, Columbia University, 2006.

[7] Muijderman, E. A., "Spiral Groove Bearings," Springer-Verlag New York 1966.

[8] Deux, A., "Design of a Silicon Microfabricated Rocket Engine Turbopump," M.S. Thesis, M.I.T., June 2001.